

Effect of Chiral Symmetry Restoration on Pentaquark Θ^+ Mass and Width at Finite Temperature and Density

Xuguang Huang ^{*}, Xuewen Hao [†], and Pengfei Zhuang [‡]

Center of Theoretical Nuclear Physics, National Laboratory of Heavy Ion Collisions, Lanzhou 730000, China
Physics Department, Tsinghua University, Beijing 100084, China

(Dated: June 21, 2018)

We investigate the effect of chiral phase transition on the pentaquark Θ^+ mass and width at one-loop level of $N\Theta^+K$ coupling at finite temperature and density. The behavior of the mass, especially the width in hadronic medium is dominated by the characteristics of chiral symmetry restoration at high temperature and high density. The mass and width shifts of positive-parity Θ^+ are much larger than that of negative-parity one, which may be helpful to determine the parity of Θ^+ in high energy nuclear collisions.

PACS numbers: 13.60.Rj, 11.10.Wx, 25.75.-q

I. INTRODUCTION

Recently, an exotic baryon Θ^+ was discovered firstly by LEPS group at Spring-8 in the reaction $\gamma n \rightarrow K^+ K^- n$ [1], and was subsequently observed by many other groups[2, 3, 4, 5, 6, 7, 8, 9, 10, 11, 12]. It has K^+n quantum numbers($B=+1$, $Q=+1$, $S=+1$), and its minimal quark content must be $uudd\bar{s}$. The remarkable features of the Θ^+ are its small mass (1540MeV) and very narrow width (<25MeV)[1]. While the isospin of Θ^+ is probably zero[4, 6, 7, 12], the other quantum numbers including spin and parity have not been measured experimentally yet. Theoretically, most of the works considers Θ^+ as a $J = \frac{1}{2}$ particle because of its low mass[13, 14, 15, 16], and some predict positive parity[13, 14, 15, 17, 18, 19, 20, 21, 22] and some suggest negative parity[16, 22, 23, 24, 25, 26, 27, 28].

The search for the pentaquark Θ^+ is also extended to the experiment of relativistic heavy ion collisions where the extreme condition to form a new state of matter – quark-gluon plasma (QGP) can be reached. The STAR collaboration[29] reported the progress of the pentaquark search in $p - p$, $d - Au$ and $Au - Au$ collisions at energy $\sqrt{s} = 200$ GeV, and the PHENIX collaboration[30] investigated the decay of the anti-pentaquark $\bar{\Theta}^+ \rightarrow K^- \bar{N}$. Theoretically, the baryon density modification[31] on the Θ^+ mass was discussed with a phenomenological density-dependent nucleon propagator[32], and the Θ^+ production in relativistic heavy ion collisions was studied in the coalescence model[33].

It is generally believed that there are two QCD phase transitions in hot and dense nuclear matter. One of them is related to the deconfinement process in moving from a hadron gas to QGP, and the other one describes the transition from the chiral symmetry breaking phase to the phase in which it is restored. From the QCD lattice simulations[34], the phase transitions are of first order in high density region and may be only a crossover in high temperature region. As the order parameter of chiral phase transition, the dynamic quark mass, or the nucleon mass reflects the characteristics of chiral symmetry restoration, and will influence the pentaquark decay process $\Theta^+ \rightarrow KN$. In this letter, we investigate the effect of chiral phase transition on the pentaquark Θ^+ mass and width at finite temperature and density at one-loop level of $N\Theta^+K$ coupling. If the mass and width shifts induced by the chiral symmetry restoration are sensitive to the pentaquark parity, it may help us to solve the puzzle of Θ^+ parity.

We proceed as follows. In Section 2, we calculate the self-energy of Θ^+ at finite temperature and density at one-loop level of pseudovector and pseudoscalar $N\Theta^+K$ couplings with positive and negative Θ^+ parity, and obtain the Θ^+ mass shift and width shift in the medium. The medium dependence of the nucleon mass is determined through the mean field gap equation of the NJL model[35] which is one of the models to see directly how the dynamical mechanisms of chiral symmetry breaking and restoration operate. In Section 3, we show the numerical calculations, analyze the contribution of chiral symmetry restoration to the mass and width shifts, and discuss the parity dependence of the results. Finally, we give our summary.

^{*} e-mail:huangxg03@mails.tsinghua.edu.cn

[†] e-mail:haoxuewen@tsinghua.org.cn

[‡] e-mail:zhuangpf@mail.tsinghua.edu.cn

II. FORMULAS

We introduce the effective Lagrangians for the pseudovector and pseudoscalar $N\Theta^+K$ couplings[32, 36],

$$\begin{aligned}\mathcal{L}_{PV} &= -\frac{g_A^*}{2f_\pi}\bar{\Theta}^+\gamma_\mu\gamma_5\partial^\mu K^+n, \\ \mathcal{L}_{PS} &= ig\bar{\Theta}^+\gamma_5K^+n.\end{aligned}\quad (1)$$

Here, the positive parity of Θ^+ is assumed. The effective lagrangians with assuming negative parity of Θ^+ can be obtained by removing $i\gamma_5$ in the vertexes. The pseudovector and pseudoscalar coupling constants g_A^* and g are fixed to reproduce the mass $M_\Theta = 1540\text{MeV}$ and decay width $\Gamma_{\Theta^+} = 15\text{ MeV}$ at zero temperature and zero density[36]. Through the calculation at tree level one has $g_A^* = 0.28$ and $g = 3.8$ for positive parity and $g_A^* = 0.16$ and $g = 0.53$ for negative parity[36].

We calculate the in-medium Θ^+ self-energy by perturbation method above mean field. To the lowest order, it is shown in Fig.1. The propagators of nucleon and kaon at mean field level read,

$$\begin{aligned}G_N(p) &= \frac{i}{p' - M_N}, \\ G_K(p) &= \frac{i}{p^2 - M_K^2},\end{aligned}\quad (2)$$

where the four-momentum p' is defined as $p' = \{p_0 + \mu, \mathbf{p}\}$ with baryon chemical potential μ . The mechanism of chiral symmetry restoration at finite temperature and density is embedded in our calculation through the effective nucleon mass M_N . Since the calculation of M_N is nonperturbative, it is difficult to calculate it directly with QCD, one has to use models. While the quantitative result depends on the models used, the qualitative temperature and density behavior is not sensitive to the details of different chiral models[37]. A simple model to describe chiral symmetry breaking in vacuum and symmetry restoration in medium is the NJL model[35]. Within this model, one can obtain the hadronic mass spectrum and the static properties of mesons remarkably well. In particular, one can recover the Goldstone mode, and some important low-energy properties of current algebra such as the Goldberger-Treiman and GellMann-Oakes-Renner relations[35]. In mean field approximation of NJL, the effective nucleon mass can be determined through the gap equation[35, 38],

$$\begin{aligned}M_N &= 3m_q, \\ 1 - \frac{N_c N_f G}{\pi^2} \int_0^\Lambda dp \frac{p^2}{E_q} \left(\tanh \frac{E_q + \mu/3}{2T} + \tanh \frac{E_q - \mu/3}{2T} \right) &= \frac{m_0}{m_q},\end{aligned}\quad (3)$$

where $E_q = \sqrt{\mathbf{p}^2 + m_q^2}$ is the constituent quark energy, the current quark mass m_0 , the color and flavor degrees of freedom N_c and N_f , the coupling constant G and the momentum cutoff Λ are chosen to fit the nucleon and pion properties in the vacuum[35, 38]. The numerical results of temperature and chemical potential dependent nucleon mass are shown in Fig.2. The effective nucleon mass drops down continuously with increasing temperature and approaches finally three times the current quark mass m_0 . Very different from the temperature effect, the nucleon mass jumps down at a critical chemical potential μ_c , which means a first-order chiral phase transition in high baryon density region. These different temperature and density effects will be reflected in the Θ^+ mass and width shifts. Considering the near cancellation of attractive scalar and repulsive vector potential, the K^+ mass increases slightly with temperature and density[37]. To simplify the calculation we take it as a constant $M_K = 494\text{ MeV}$ in the following.

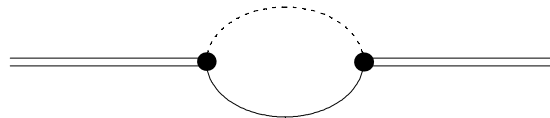


FIG. 1: The lowest order Θ^+ self-energy. The solid and dashed line represent nucleon and kaon field, respectively.

The Θ^+ self-energy can be separated into a scalar and a vector part,

$$\Sigma(p') = \Sigma_s(p') + \Sigma_\mu(p')\gamma^\mu, \quad (4)$$

with which the propagator of Θ^+ reads

$$G_\Theta = \frac{i}{p'^\mu\gamma_\mu - m_\Theta - \Sigma} = i \frac{(p'^\mu - \Sigma^\mu)\gamma_\mu + (m_\Theta + \Sigma_s)}{(p'^\mu - \Sigma^\mu)(p'_\mu - \Sigma_\mu) - (m_\Theta + \Sigma_s)^2}, \quad (5)$$

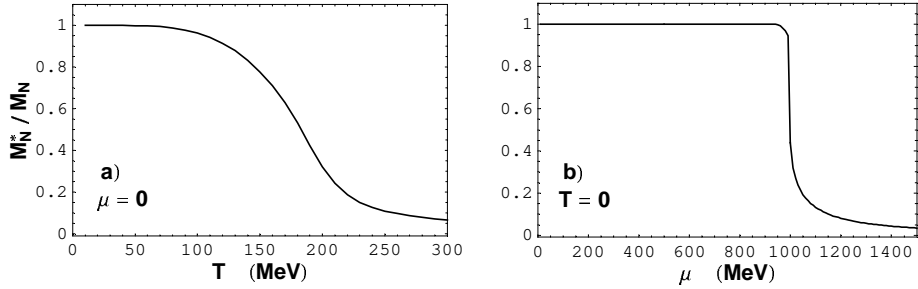


FIG. 2: The effective nucleon mass scaled by its value in the vacuum as a function of temperature at zero chemical potential (a) and a function of chemical potential at zero temperature (b).

where m_Θ is the Θ^+ mass in vacuum. The Θ^+ complex mass $\mathcal{M}_\Theta = M_\Theta - i\frac{\Gamma}{2}$ in the medium can be determined by the pole equation of the propagator,

$$[(p'^\mu - \Sigma^\mu)(p'_\mu - \Sigma_\mu) - (m_\Theta + \Sigma_s)^2] \Bigg|_{p'_0 = \sqrt{\mathcal{M}_\Theta^2 + \mathbf{p}^2}} = 0. \quad (6)$$

From this equation, one can obtain the temperature, chemical potential, and momentum dependence of the Θ^+ mass and width.

In the rest frame of Θ^+ , $\mathbf{p} = 0$ and $\mathbf{\Sigma} = 0$, the calculation can be done more easily. Since the width of Θ^+ is very small compared to its mass (we assume that this statement holds both in vacuum and in medium), the Eq.(6) can be separated into two uncoupled equations. The pentaquark mass M_Θ at finite temperature and density is calculated through the gap equation

$$M_\Theta = m_\Theta + \text{Re}(\Sigma_0(M_\Theta) + \Sigma_s(M_\Theta)), \quad (7)$$

and the medium correction to the pentaquark width Γ is determined by

$$\Delta\Gamma_\Theta = -2\text{Im}(\Sigma_0(M_\Theta) + \Sigma_s(M_\Theta)). \quad (8)$$

For the pseudovector coupling with positive parity,

$$\begin{aligned} -i\Sigma^{PV}(p) &= -\left(\frac{g_A^*}{2f_\pi}\right)^2 \int \frac{d^4k}{(2\pi)^4} (\not{p} - \not{k}) \frac{\not{k}' - M_N}{\not{k}'^2 - M_N^2} \frac{1}{(p - k)^2 - M_K^2} (\not{p} - \not{k}) \\ &= \left(\frac{g_A^*}{2f_\pi}\right)^2 \int \frac{d^4k}{(2\pi)^4} \frac{M_N(p - k)^2 - 2k' \cdot (p - k)p' + (p'^2 - k'^2)\not{k}'}{(\not{k}'^2 - M_N^2)((p - k)^2 - M_K^2)}. \end{aligned} \quad (9)$$

where k is the loop 4-momentum carried by the nucleon. Taking the transformations $\int \frac{dk_0}{(2\pi)} \rightarrow iT \sum_m$ and $k_0 \rightarrow i\omega_m$ in imaginary time formalism of finite temperature field theory, we can obtain the explicit expression of Θ^+ self-energy at finite temperature and density, where $\omega_m = (2m + 1)\pi T$ with $m = 0, \pm 1, \pm 2, \dots$ is the fermion frequency. After the summation over the nucleon frequency one derives the real and imaginary parts of the in-medium self-energy,

$$\begin{aligned} \text{Re}\Sigma_s^{PV}(M_\Theta) &= -\frac{1}{2} \left(\frac{g_A^*}{2f_\pi}\right)^2 \int \frac{d^3\mathbf{k}}{(2\pi)^3} \frac{M_N}{E_N} \left[\left(1 + \frac{M_K^2}{F_-(N, K)}\right) f_f^- + \left(1 + \frac{M_K^2}{F_+(N, K)}\right) f_f^+ \right. \\ &\quad \left. - M_K^2 \frac{E_N}{E_K} \left(\frac{1}{F_+(K, N)} + \frac{1}{F_-(K, N)}\right) f_b \right], \\ \text{Re}\Sigma_0^{PV}(M_\Theta) &= \frac{1}{2} \left(\frac{g_A^*}{2f_\pi}\right)^2 \int \frac{d^3\mathbf{k}}{(2\pi)^3} \left[\left(1 + \frac{E_N M_K^2 + 2M_\Theta \mathbf{k}^2}{E_N F_-(N, K)}\right) f_f^- - \left(1 + \frac{E_N M_K^2 - 2M_\Theta \mathbf{k}^2}{E_N F_+(N, K)}\right) f_f^+ \right. \\ &\quad \left. - \left(\frac{M_\Theta(E_K^2 + \mathbf{k}^2)}{E_K E_N}\right) \left(\frac{M_\Theta - E_N}{F_-(N, K)} - \frac{M_\Theta + E_N}{F_+(N, K)}\right) - \frac{E_K M_K^2}{E_N} \left(\frac{1}{F_-(N, K)} - \frac{1}{F_+(N, K)}\right)\right) f_b \right] \end{aligned} \quad (10)$$

and

$$\text{Im}\Sigma_s^{PV}(M_\Theta) = \frac{\pi M_N M_K^2}{4} \left(\frac{g_A^*}{2f_\pi}\right)^2 \int \frac{d^3\mathbf{k}}{(2\pi)^3} \frac{1}{E_K E_N} \left[(\delta_-(K, N) - \delta_+(K, N)) f_f^- + \delta_+(N, K) f_f^+ \right]$$

$$\begin{aligned}
& - (\delta_+(K, N) + \delta_-(K, N) - \delta_+(N, K)) f_b \Big] , \\
Im\Sigma_0^{PV}(M_\Theta) &= -\frac{\pi}{4} \left(\frac{g_A^*}{2f_\pi} \right)^2 \int \frac{d^3\mathbf{k}}{(2\pi)^3} \frac{1}{E_N E_K} \left[(E_N M_K^2 + 2M_\Theta \mathbf{k}^2) (\delta_-(K, N) - \delta_+(K, N)) f_f^- \right. \\
& - (E_N M_K^2 - 2M_\Theta \mathbf{k}^2) \delta_+(N, K) f_f^+ \\
& - \left(\frac{M_\Theta (E_K^2 + \mathbf{k}^2) (M_\Theta - E_N) - E_K^2 M_K^2}{E_K} (\delta_-(K, N) - \delta_+(K, N)) \right. \\
& \left. \left. - \frac{M_\Theta (E_K^2 + \mathbf{k}^2) (M_\Theta + E_N) - E_K^2 M_K^2}{E_K} \delta_+(N, K) \right) f_b \right] , \tag{11}
\end{aligned}$$

with particle energies

$$E_N^2 = \mathbf{k}^2 + M_N^2 , \tag{12}$$

$$E_K^2 = \mathbf{k}^2 + M_K^2 , \tag{13}$$

the Fermi-Dirac and Bose-Einstein distributions

$$f_f^\pm = \frac{1}{e^{(E_N \pm \mu)/T} + 1} , \tag{14}$$

$$f_b = \frac{1}{e^{E_K/T} - 1} , \tag{15}$$

and the functions $F_\pm(X, Y)$ and $\delta_\pm(X, Y)$ defined by

$$\begin{aligned}
F_\pm(X, Y) &= (M_\Theta \pm E_X)^2 - E_Y^2 , \\
\delta_\pm(X, Y) &= \delta(M_\Theta \pm E_X - E_Y) . \tag{16}
\end{aligned}$$

For the pseudoscalar coupling with positive parity,

$$\begin{aligned}
Re\Sigma_s^{PS}(M_\Theta) &= -\frac{g^2 M_N}{2} \int \frac{d^3\mathbf{k}}{(2\pi)^3} \left[\frac{1}{E_N} \left(\frac{1}{F_-(N, K)} f_f^- + \frac{1}{F_+(N, K)} f_f^+ \right) - \frac{1}{E_K} \left(\frac{1}{F_-(K, N)} + \frac{1}{F_+(K, N)} \right) f_b \right] , \\
Re\Sigma_0^{PS}(M_\Theta) &= \frac{g^2}{2} \int \frac{d^3\mathbf{k}}{(2\pi)^3} \left[\frac{1}{F_-(N, K)} f_f^- - \frac{1}{F_+(N, K)} f_f^+ - \frac{1}{E_K} \left(\frac{M_\Theta - E_K}{F_-(K, N)} + \frac{M_\Theta + E_K}{F_+(K, N)} \right) f_b \right] , \tag{17}
\end{aligned}$$

and

$$\begin{aligned}
Im\Sigma_s^{PS}(M_\Theta) &= \frac{\pi g^2 M_N}{4} \int \frac{d^3\mathbf{k}}{(2\pi)^3} \frac{1}{E_K E_N} \left[(\delta_-(K, N) - \delta_+(K, N)) f_f^- + \delta_+(N, K) f_f^+ \right. \\
& \left. - (\delta_+(K, N) + \delta_-(K, N) - \delta_+(N, K)) f_b \right] , \\
Im\Sigma_0^{PS}(M_\Theta) &= -\frac{\pi g^2}{4} \int \frac{d^3\mathbf{k}}{(2\pi)^3} \frac{1}{E_K} \left[(\delta_-(K, N) - \delta_+(K, N)) f_f^- - \delta_+(N, K) f_f^+ \right. \\
& \left. - \left(\frac{M_\Theta - E_K}{E_N} (\delta_-(K, N) - \delta_+(N, K)) + \frac{M_\Theta + E_K}{E_N} \delta_+(K, N) \right) f_b \right] . \tag{18}
\end{aligned}$$

For the couplings with negative Θ^+ parity, the only difference is to change the sign of the corresponding scalar self energy, $\Sigma_s^{PV} \rightarrow -\Sigma_s^{PV}$ and $\Sigma_s^{PS} \rightarrow -\Sigma_s^{PS}$. We will see in the following that this change in sign leads to a partial cancellation between Σ_0 and Σ_s in determining the in-medium Θ^+ mass and width, and results in small mass and width shifts for negative-parity Θ^+ .

III. NUMERICAL RESULTS

With the formulas given in last section, we now calculate numerically the Θ^+ mass shift $\Delta M_\Theta(T, \mu) = M_\Theta(T, \mu) - m_\Theta$ and the width shift $\Delta\Gamma(T, \mu)$ at finite temperature and density for the pseudovector (PV) and pseudoscalar (PS) couplings with positive and negative Θ^+ parity. We call these four couplings in the following PV^+, PV^-, PS^+, PS^- , respectively.

We first consider the mass shift. From its temperature dependence at fixed chemical potentials (Figs.3a and b) and chemical potential dependence at fixed temperatures (Figs.3c and d), it has the following properties:

1) The Θ^+ becomes light in the medium, like most of the hadrons such as nucleon, ρ meson and σ meson characterized by chiral symmetry. While for the couplings PS^- , PV^- and PV^+ the mass shift by pure temperature effect is rather small, see Fig.3a, it becomes remarkable in the case with high baryon density and high temperature, see Figs.3b-d.

2) The temperature and density dependence of the mass shift is controlled by the chiral properties. In the case of pure temperature effect (Fig.3a) and the case of high temperature and high density effect (Figs.3b and d), the continuous chiral phase transition, shown in Fig.2a for $\mu = 0$, results in a smooth mass shift. In the case of high density but low temperature, the mass shift is zero in the chiral breaking phase at $\mu < \mu_c$, changes suddenly at the phase transition with $\mu = \mu_c$, and decreases rapidly in the chiral restoration phase with $\mu > \mu_c$, see Fig.4c. This behavior reflects the properties of first-order chiral phase transition shown in Fig.2b.

3) The degree of the Θ^+ mass change depends strongly on its parity. In any case of temperature and density, the mass shift of positive-parity Θ^+ is much larger than that of negative-parity one. For instance, at $T = 200$ MeV and $\mu = 1000$ MeV, the mass shifts for the couplings PS^+ , PV^+ , PV^- and PS^- are, respectively, -115 , -40 , -10 and -2 MeV.

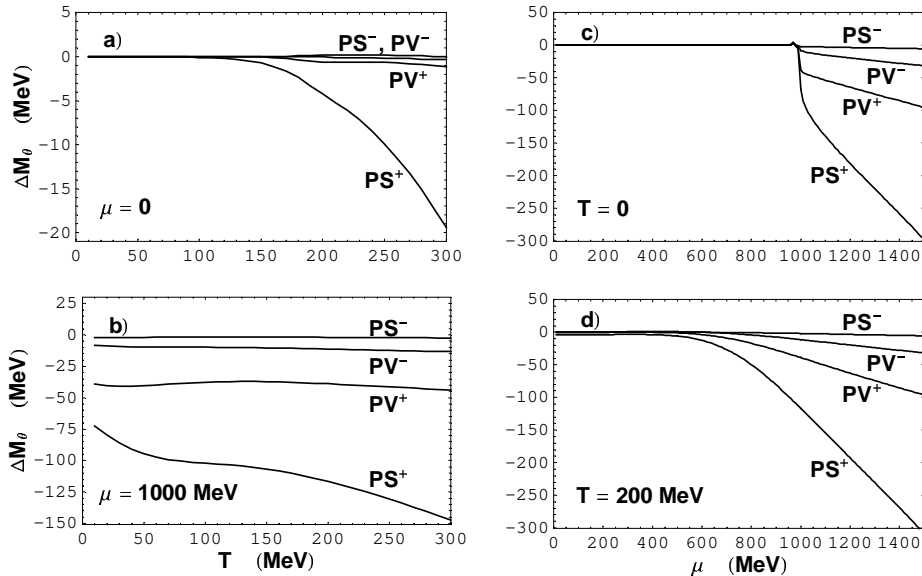


FIG. 3: The temperature dependence at fixed chemical potentials $\mu = 0$ (a) and $\mu = 1000$ MeV (b) and the chemical potential dependence at fixed temperatures $T = 0$ (c) and $T = 200$ MeV (d) of the Θ^+ mass shift for four different couplings.

We turn to the discussion of the Θ^+ width shift. It is indicated as a function of temperature at fixed chemical potentials (Figs.4a and b) and a function of chemical potential at fixed temperatures (Fig.4c and d) for the four different couplings. Related to the properties of the mass shift, the width has the characteristics:

- 1) Like most of the hadrons in medium, the suppressed mass leads to Θ^+ broadening at finite temperature and density. The pentaquark will become more and more unstable with increasing temperature and density, and easy to decay in relativistic heavy ion collisions if it is created.
- 2) Again, the behavior of the width shift is dominated by the chiral properties. The width increases continuously in the case of pure temperature effect and the case of high density and high temperature, but starts to jump up suddenly at the critical chemical potential μ_c in the case of high density but low temperature, resulted from the chiral phase transition shown in Fig.2.
- 3) The broadening depends also on the Θ^+ parity. In any case the broadening of positive-parity Θ^+ is much larger than that of negative-parity one.
- 4) Compared with the vacuum mass and width (1540 MeV and 15 MeV in our calculation), the mass shift is slight, but the width shift is extremely strong. From Fig.3 the maximum mass shift in the considered temperature and density region is 20% of the vacuum value for the coupling PS^+ and 6% for the coupling PV^+ . However, from the Fig.4 the maximum width shift is 17 times the vacuum value for PS^+ and 7 times for PV^+ !

To study the pentaquark production in relativistic heavy ion collisions, we estimate the Θ^+ mass and width shifts at RHIC, SPS and SIS, shown in Tab.I. We take the corresponding temperature and baryon chemical potential at RHIC, SPS and SIS as $(T, \mu) = (200, 50), (180, 300)$ and $(150, 700)$ MeV, respectively. While the mass shift can be neglected in any case, the width shift for positive-parity Θ^+ at SPS and SIS is important and measurable. Compared with the width shift in the vacuum, it goes up from 7% at RHIC to 40% at SPS and to 380% at SIS for the coupling PV^+ , and from 23% at RHIC to 70% at SPS and to 760% at SIS for the coupling PS^+ !

The temperature and density are introduced into our calculation through two ways. One is the chiral symmetry restoration reflected in the effective nucleon mass, and the other one is the loop frequency summation in Fig.1. To make sure that the remarkable mass shift and the crucial width shift are induced mainly by the chiral properties,

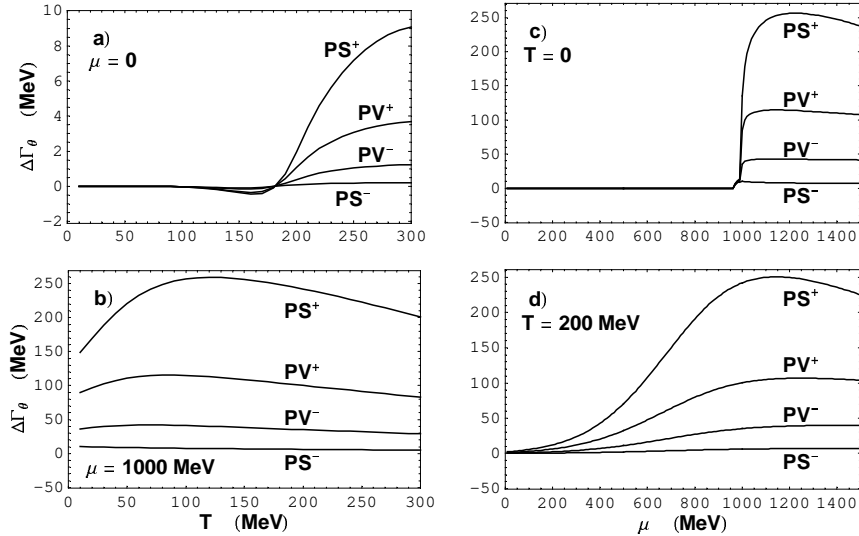


FIG. 4: The temperature dependence at fixed chemical potentials $\mu = 0$ (a) and $\mu = 1000\text{MeV}$ (b) and the chemical potential dependence at fixed temperatures $T = 0$ (c) and $T = 200\text{MeV}$ (d) of the Θ^+ width shift for four different couplings.

	T	μ	ΔM_Θ				$\Delta \Gamma_\Theta$			
			PV^+	PV^-	PS^+	PS^-	PV^+	PV^-	PS^+	PS^-
RHIC	200	50	-0.5	0.2	-4.0	0	1.1	0.7	3.5	0.2
SPS	180	300	-0.6	0.4	-2.8	0.1	6.4	2.4	10.5	0.7
SIS	150	700	-4.0	1.0	-9.4	0.2	57.6	20.3	115.1	4.4

TABLE I: The estimation of Θ^+ mass and width shifts at RHIC, SPS and SIS for four different couplings.

we now turn off the way of chiral phase transition and keep the nucleon mass as the vacuum value $M_N = 940\text{MeV}$ during the numerical calculation. The results are shown in Fig.5. Compared with the calculation with chiral symmetry restoration, at zero chemical potential the maximum mass shift is reduced from -20 MeV (Fig.3a) to -10 MeV (Fig.5a), and the maximum width shift is strongly suppressed from 9 MeV (Fig.4a) to -1 MeV (Fig.5b). Qualitatively different from the case with chiral symmetry restoration, the Θ^+ becomes narrow in the case without chiral symmetry restoration. It is easy to see that the considerable mass shift, especially the extreme width shift are originated from the mechanism of chiral phase transition.

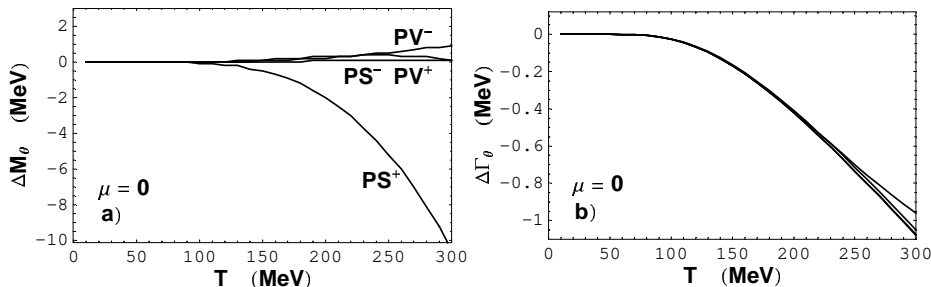


FIG. 5: The temperature dependence of the Θ^+ mass shift (a) and width shift (b) with a constant nucleon mass for four different couplings.

IV. CONCLUSIONS

We studied the temperature and density effect on the pentaquark mass and width to the lowest order of the perturbation expansion above chiral mean field for four different $N\Theta^+K$ couplings. The chiral phase transition, here reflected in the effective nucleon mass, plays an essential rule in determining the in-medium Θ^+ mass and width shifts. Like most of the hadrons, the Θ^+ becomes light and unstable in high temperature and density region where the chiral symmetry is restored. The degree of the mass and width shifts depends strongly on the Θ^+

parity. For positive-parity Θ^+ , the maximum width shift in reasonable temperature and density region is 17 times its vacuum value for pseudoscalar coupling, and 7 times for pseudovector coupling, while for negative-parity Θ^- , the width shift is much smaller. This parity dependence may be helpful to determine the pentaquark parity in relativistic heavy ion collisions. At SIS energy, the width shift is almost 4-8 times the vacuum value for positive-parity Θ^+ . When the chiral symmetry restoration is removed from the calculation, the pure temperature and density effect resulted from the thermal loop on the mass and width becomes rather small.

Acknowledgments: The work is supported in part by the Grants NSFC10135030 and G2000077407.

[1] T. Nakano et al., Phys. Rev. Lett. **91**, (2003) 012002.
 [2] V. V. Barmin et al., Phys. Atom. Nucl. **66** (2003) 1715.
 [3] S. Stepanyan et al., Phys. Rev. Lett. **91** (2003) 252001.
 [4] J. Barth et al., Phys. Lett. **B572** (2003) 127.
 [5] A. E. Aratayn, A. G. Dololenko and M. A. Kubantsev, Phys. Atom. Nucl. **67** (2004) 682.
 [6] V. Kubarovskiy et al., Phys. Rev. Lett. **92** (2004) 032001.
 [7] A. Airapetian et al., Phys. Lett. **B585** (2004) 213.
 [8] SVD Collaboration, hep-ex/0401024.
 [9] COSY-TOF Collaboration, Phys. Lett. **B595** (2004) 127.
 [10] P. Zh. Aslanyan et al., hep-ex/0403044.
 [11] ZEUS Collaboration, Phys. Lett. **B591** (2004) 7.
 [12] S. V. Chekanov, hep-ex/0404007.
 [13] D. Diakonov, V. Petrov, and M. Polyakov, Z. Phys. **A 359**, (1997) 305.
 [14] R. Jaffe and F. Wilczek, Phys. Rev. Lett. **91**, (2003) 232003.
 [15] F. Stancu and D. O. Riska, Phys. Lett. **B575** (2003) 242.
 [16] F. Huang, Z. Y. Zhang, Y. W. Yu, and B. S. Zou, Phys. Lett. **B586** (2004) 69.
 [17] T.-W. Chiu, and T.-H. Hsieh, hep-ph/0403020.
 [18] M. Karliner and H. J. Lipkin, hep-ph/0307243.
 [19] A. Hosaka, Phys. Lett. **B571** (2003) 55.
 [20] C. E. Carlson, C.D. Carone, H.J. Kwee, V. Nazaryan, Phys. Rev. **D 70** (2004) 0375001.
 [21] Y.-X. Liu, J.-S. Li, and C.-G. Bao, hep-ph/0401197.
 [22] N. Mathur, F.X. Lee, A. Alexandru, A. Bennhold, and Y. Chen, Phys. Rev. **D 70** (2004) 074508.
 [23] F. Csikor et al., JHEP **0311** (2003) 070; S. Sasaki, Phys. Rev. Lett. **93** (2004) 152001.
 [24] S.-L. Zhu, Phys. Rev. Lett. **91**, (2003) 232002.
 [25] R.D. Matheus et al., Phys. Lett. **B578** (2004) 323; J. Sugiyama et al., Phys. Lett. **B581** (2004) 167.
 [26] C. E. Carlson et al., Phys. Lett. **B 573**, (2003) 101.
 [27] B. Wu and B.-Q. Ma, hep-ph/0311331.
 [28] X.-C. Song and S.-L. Zhu, Mod. Phys. Lett. **A 19** (2004) 2791-2797.
 [29] S. Salur (for the STAR collaboration), nucl-ex/0403009.
 [30] C. Pinkenburg (for the PHENIX collaboration), J. Phys. **G30** (2004) s1201.
 [31] F.S. Navarra, M. Nielsen and K. Tsushima, nucl-th/0408072.
 [32] H. -Ch. Kim, C. -H. Lee, and H. -J. Lee, hep-ph/0402141.
 [33] L. W. Chen, V. Greco, C. M. Ko, S. H. Lee, and W. Liu, Phys. Lett. **B 601** (2004) 34-40.
 [34] see, for instance, Z. Fodor, and S. D. Katz, JHEP **0404** (2004) 050.
 [35] see, for instance, U. Vogl and W. Weise, Prog. Part. and Nucl. Phys. **27** (1991) 195; S. P. Klevansky, Rev. Mod. Phys. **64** (1992) 649.
 [36] S. I. Nam, A. Hosaka, and H. -Ch. Kim, Phys. Lett. **B 579**, (2004) 43.
 [37] see, for instance, G. Q. Li, nucl-th/9710008.
 [38] P. Zhuang, J. Hüfner, and S. P. Klevansky, Nucl. Phys. **A576** (1994) 525.